AFRL-OSR-VA-TR-2014-0193

THE NEURONAL CONTROL OF FLYING PREY INTERCEPTION IN DRAGONFLIES

Robert Olberg
TRUSTEES OF UNION COLLEGE IN THE TOWN OF SCHENECTADY IN THE STATE OF NEW YORK

08/19/2014
Final Report

Air Force Research Laboratory
AF Office Of Scientific Research (AFOSR)/ RTC
Arlington, Virginia 22203
Air Force Materiel Command

REPORT DOCUMENTATION PAGE	*Form Approved* *OMB No. 0704-0188*

1. REPORT DATE *(DD-MM-YYYY)* 12-08-2014	**2. REPORT TYPE** Final	**3. DATES COVERED** *(From - To)* 15-05-2010 to 14-05-2014

4. TITLE AND SUBTITLE The neuronal control of flying prey interception in dragonflies	**5a. CONTRACT NUMBER**
	5b. GRANT NUMBER FA9550-10-1-0472
	5c. PROGRAM ELEMENT NUMBER
6. AUTHOR(S) Olberg, Robert M. Gonzalez-Bellido, Paloma Wardill, Trevor	**5d. PROJECT NUMBER**
	5e. TASK NUMBER
	5f. WORK UNIT NUMBER
7. PERFORMING ORGANIZATION NAME(S) AND ADDRESS(ES) Union College 807 Union Street Schenectady, NY 12308 USA	**8. PERFORMING ORGANIZATION REPORT NUMBER**
9. SPONSORING/MONITORING AGENCY NAME(S) AND ADDRESS(ES) AIR FORCE OFFICE OF SCIENTIFIC RESEARCH	**10. SPONSOR/MONITOR'S ACRONYM(S)** AFOSR/PKR1
	11. SPONSOR/MONITOR'S REPORT NUMBER(S) DUNS143574726

12. DISTRIBUTION/AVAILABILITY STATEMENT

Distribution A. Approved for public release

13. SUPPLEMENTARY NOTES

14. ABSTRACT

Eight pairs of large descending visual neurons (TSDNs) control dragonfly prey interception flights. We investigated both the sensory inputs and the motor outputs of this group of neurons. A detailed map was obtained of the position and direction of target movement that excites each of the TSDNs. This study also revealed the anatomy of the TSDN output terminals, providing information about the likely pattern of connectivity from individual TSDNs to the neural circuitry controlling each of the wings. Angular speed is also encoded by the TSDNs. This speed sensitivity increases the gain of the system as the dragonfly approaches its prey. Distance appears not to be encoded by the TSDNs when the head is fixed. However binocular inputs are required for maximal responses. The functional implication of the binocular inputs is not yet known. Intracellular electrical stimulation of individual TSDNs confirmed their role in adjusting wing position and angle. TSDN activity rotates the head as well in the direction opposite the preferred target direction. Two TSDNs also move the legs and mouthparts.

15. SUBJECT TERMS

Insect flight, Prey interception, Insect vision, Receptive field, Dragonfly

16. SECURITY CLASSIFICATION OF:			**17. LIMITATION OF ABSTRACT**	**18. NUMBER OF PAGES**	**19a. NAME OF RESPONSIBLE PERSON** Robert M. Olberg
a. REPORT	**b. ABSTRACT**	**c. THIS PAGE**			
U	U	U	UU	0	**19b. TELEPHONE NUMBER** *(Include area code)* 518 388 6509

THE NEURONAL CONTROL OF FLYING PREY INTERCEPTION IN DRAGONFLIES
Final Report

Introduction

This project focused on a complex behavior, flying prey interception by dragonflies, and on 8 pairs of large, anatomically identified neurons called Target Selective Descending Neurons (TSDNs – Olberg 1986) that are implicated in controlling this behavior. These neurons show directionally selective responses to object movement, but not to wide field or whole animal movement. Their receptive fields are in the dorsal frontal quadrant of vision, the direction of the prey's image during dragonfly approach. Electrical stimulation of these neurons individually elicits wing movement, suggesting that they are involved in steering flight with respect to moving objects. Dragonflies sustain themselves by capturing and consuming flying prey; all of the properties of the TSDNs suggest that they comprise the primary pathway from the brain to the thorax for the control of prey interception.

The first objective in this project was to quantify in greater detail the visual and multisensory inputs to the two sets of descending neurons, Target Selective Descending Neurons (TSDNs – Olberg 1986, Frye and Olberg 1995) and Rotation Sensitive Descending Neurons (RSDNs – Olberg 1981). The second objective was to investigate the outputs of the flight control neurons, comparing the wing movements produced by stimulating the neurons electrically with movements elicited with visual and mechanosensory stimulation. The third and most ambitious objective was to monitor the activity of the flight control neurons in free foraging flight, as the dragonfly intercepts its prey. As will be detailed below, there was significant progress in all of these areas during the 4-year grant period.

1. Visual inputs to the descending neurons controlling flight.

A. TSDN receptive fields and population coding of target direction

Considerable progress was achieved in this aspect of the project, specifically with respect to the visual receptive fields of the TSDNs. With Dr. Paloma Gonzalez-Bellido, a major effort was put into a detailed receptive-field investigation of the TSDNs. (Dr. Gonzalez-Bellido was a research assistant with Dr. Anthony Leonardo, a group leader at the Howard Hughes Medical Institute research campus at Janelia Farm. Dr. Gonzalez-Bellido's and Dr. Trevor Wardill's work with killer-fly predation flight trajectories was also funded by a supplement to this grant – see section 4 below.) Using small targets presented at random locations and moving in random directions over long periods of time (hours), Dr. Gonzalez-Bellido was able to obtain much higher resolution maps of TSDN visual responses than were previously available (Fig. 1). In collaboration with Dr. Apostalos Georgopoulos, an expert in neuronal population coding in the primate brain, it was determined the TSDN population vector accurately codes target movement direction within a few degrees (Fig. 2). At the same time Dr. Gonzalez-Bellido's fluorescent dye (Lucifer-yellow) injections illuminated for the first time the anatomy of the output regions of the TSDNs, providing information about the likely pattern of connectivity from individual TSDNs to the wing-control neuropils (Fig. 3). The paper presenting this work (Gonzalez-Bellido et al. 2012) won the Proceedings of the National Academy of Sciences annual Cozzarelli prize for best paper in the Biological Sciences.

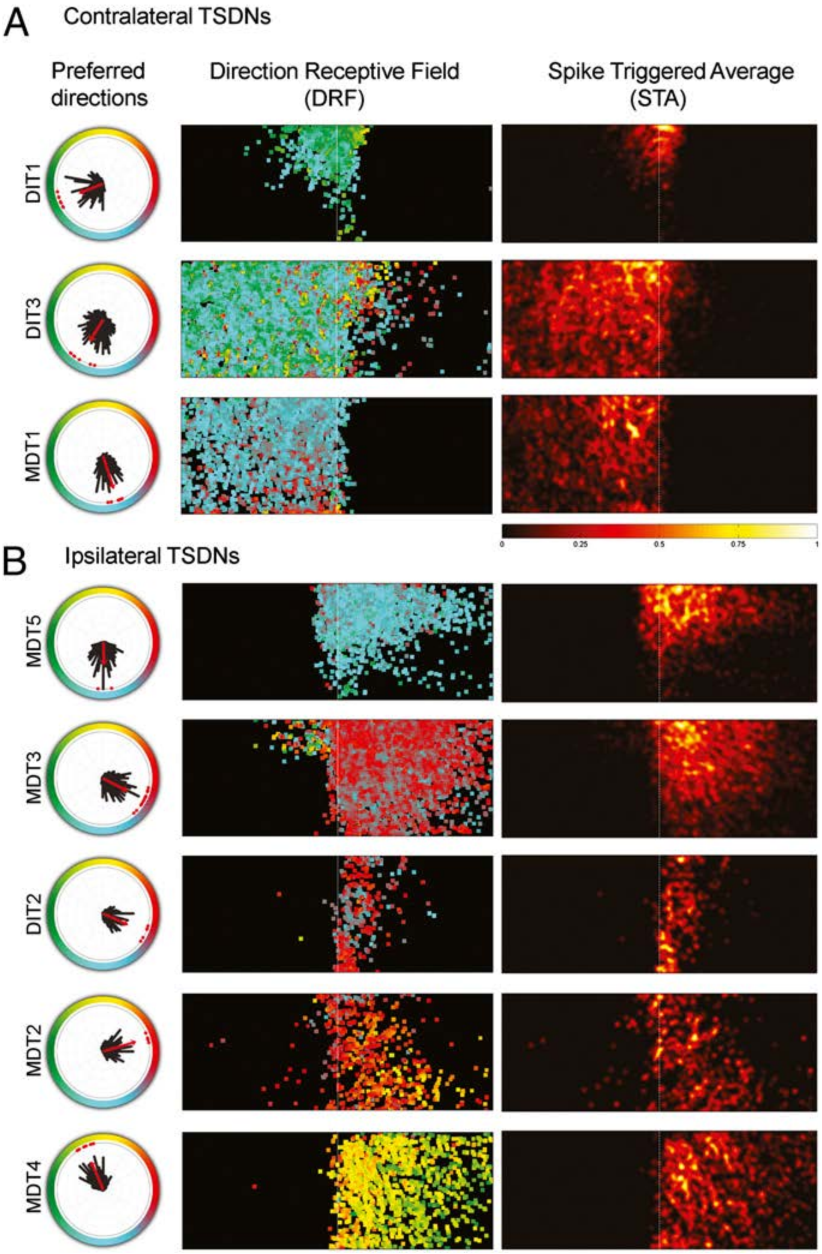

Fig. 1. Each TSDN type shows a unique direction tuning curve and receptive field consistent across animals. (A) Contralateral and (B) ipsilateral TSDN receptive fields whose axons were in the right connective of the ventral nerve cord (VNC). The polar plots show the directional preference of each recorded TSDN (red dots) and their mean direction tuning distribution (black bars). The red arrow indicates mean preferred direction. The color-coded direction receptive field (DRF) maps show the mean direction preference at each pixel, which was calculated by averaging the direction peak, at each pixel, for all recordings of each TSDN type. In addition, spike-triggered average (STA) maps are shown for each TSDN type. Note that, because number of spikes was normalized before and after computing the average, the same scale applies to all STA maps. *Figure and*

caption reproduced from Gonzalez-Bellido 2012.

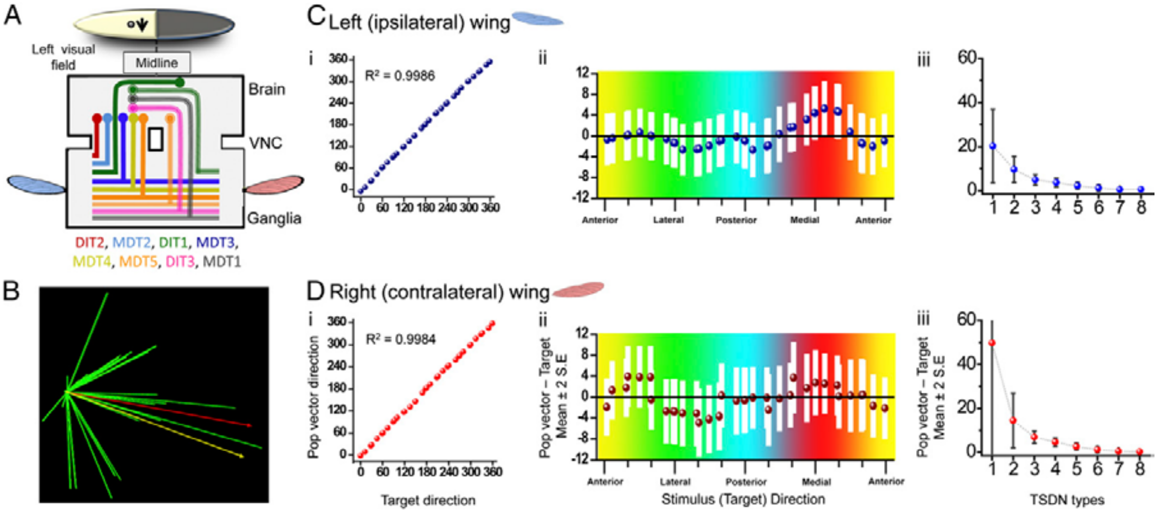

Fig. 2. The TSDN population vector codes direction of the prey with high accuracy. (A) A target moving in the left side of the visual field activates the subset of TSDNs shown in the diagram. The population of TSDNs providing inputs to the left (nine cells) and right (seven cells) wings differ. (B) Graphical representation of a dragonfly TSDN population vector. Contributing TSDN vectors (green), stimulus direction (yellow), and population vector (red) are shown. (C and D) Population vectors for the left (C) and right (D) wings were calculated for all presented trajectories. (C, i and D, i) The population vectors, binned in 18°, are strongly correlated with the target direction. Left wing circular R = 0.9986 (P < 0.001) and right wing R = 0.9984 (P < 0.001). (C, ii and D, ii) The direction of the target and the direction of the population vector are not significantly different in any direction because the difference between these two parameters is close to zero (dotted values) and because zero is within the 95% confidence interval (white bars). Colors refer to the direction of the presented target. The data concern targets moving in the left side of the visual field, so targets that traveled toward the medial part of the animal correspond to the red section. (C, iii and D, iii) On average, removing two types of TSDN from the population (six cell types used) does not impact the accuracy of the population vector significantly. For the left wing, three TSDN types are, on average, sufficient to provide a population vector whose bias is within 10° of the presented target direction. *Figure and caption reproduced from Gonzalez-Bellido et al. 2012.*

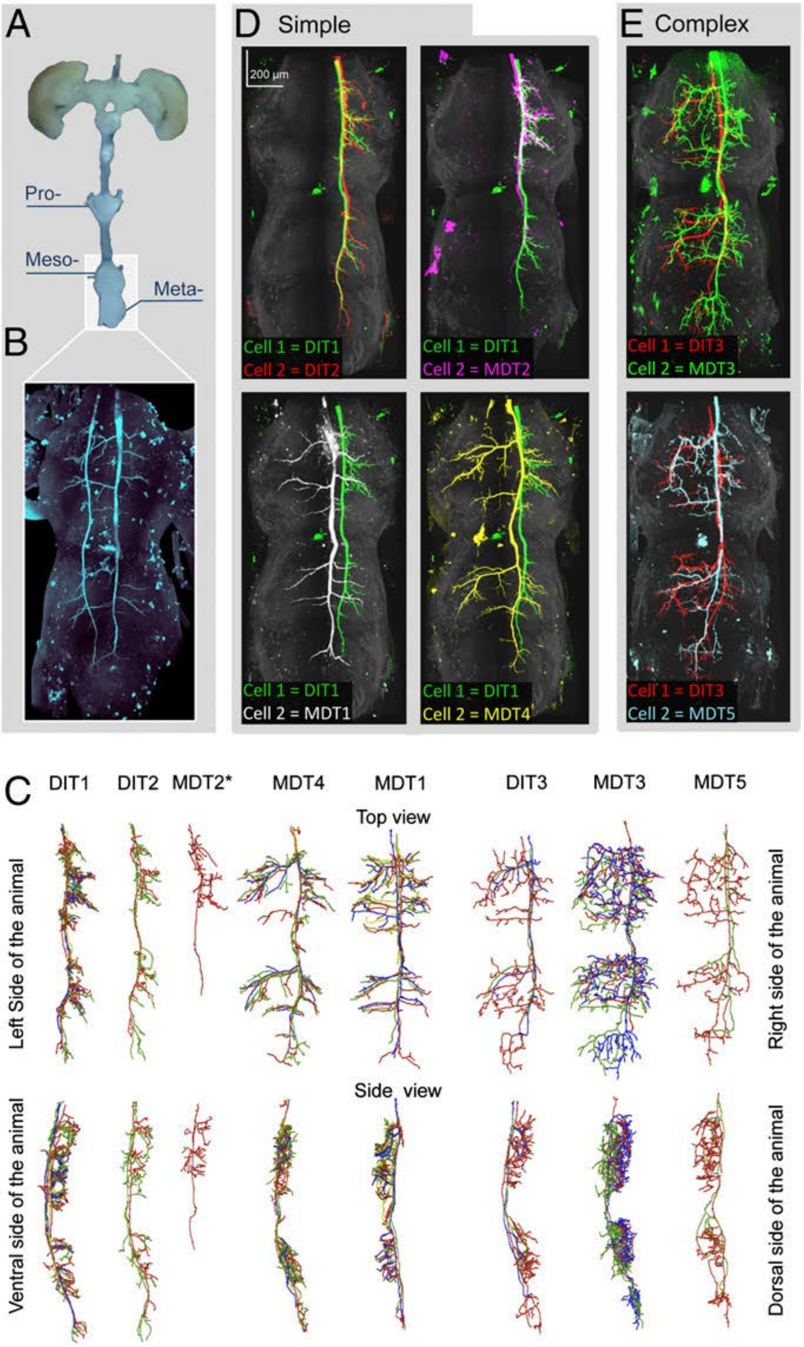

Fig. 3. In the wing motor centers, all TSDNs share morphological features. (A) The mesothoracic, metathoracic, and first abdominal ganglia were imaged and warped to allow morphological comparison. (B) Unilateral DIT2 on the left and bilateral MDT1 on the right, injected in the same animal, target the same locations. (C) Traces within each TSDN type (grouped according to the electrophysiological results) are consistent, so the most complete fill from each TSDN type was used for comparison. TSDNs were categorized into “simple” or “complex” cells. A pairwise comparison (dorsal views) shows that unilateral simple cells, DIT1 (green), DIT2 (red), and MDT2 (magenta), are indistinguishable from each other (D, Upper), but the bilateral simple cells MDT1 (white) and MDT4 (yellow) display specific branching patterns (D, Lower). However, all simple TSDNs target the same location. In contrast, pairwise comparisons be- tween the complex cells, DIT3 (red), MDT3 (green), and MDT5 (cyan) (E, all panels) are less informative because their additional intricate branching exhibits higher variability, particularly in the medial region of the ganglia (traces in C).

Figure and caption reproduced from Gonzalez-Bellido 2012

B. 3-Dimensional Receptive Field Study and the coding of target distance

Earlier observations from outdoor TSDN recordings to real moving objects suggested that these neurons might be sensitive to object distance. Two sets of experiments were carried out to determine whether the TSDNs encode target distance as well as target direction and position. For the first study, a robotic 3-dimensional prey simulator was designed and built by Union College undergraduate engineering majors, Max Balter and Adam Zinman, under the direction of Dr. David Hodgson, in Union's mechanical engineering department. (These students were supported by summer-research fellowships provided by this AFOSR award.) The prey-motion simulator, shown in Figure 4, was designed to produce movements of a small bead mounted on fine nylon monofilament. Movement is generated by DC motors with feedback control via built-in optical encoders. Three-dimensional motion is controlled by MatLab software.

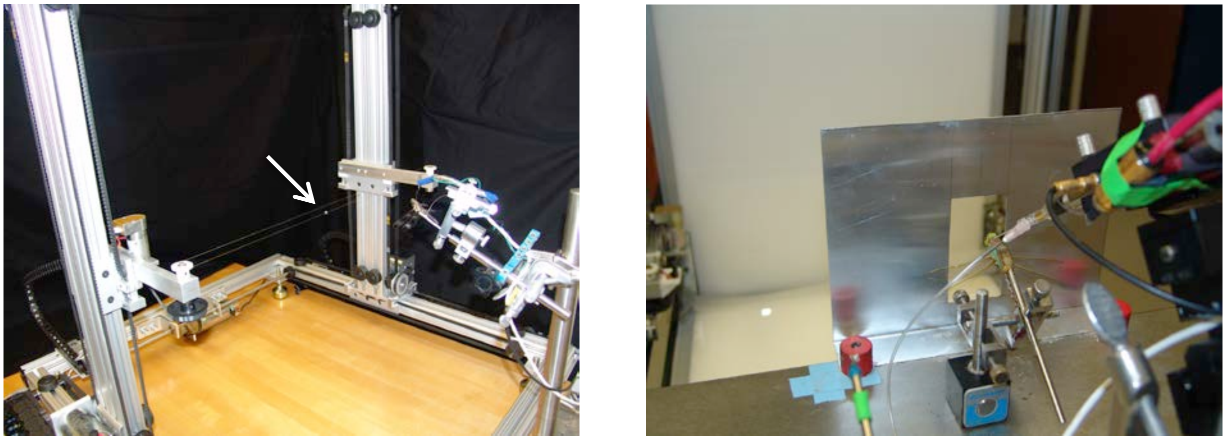

Fig. 4. Two views of 3-dimensional prey-motion simulator. Left panel shows early recording with dragonfly viewing moving bead (arrow) but also movement of the carriages. Right panel shows more recent recording with dragonfly viewing bead movement through a window to eliminate view of carriages and with LED panels providing a bright background.

To date we have recorded the responses of 5 different TSDNs (each more than once) to simulated prey motion in 3 dimensions. An example of the results for one of the TSDNs, DIT1, (Fig. 5) represents the common trend seen for all of the neurons. The neurons spiked most to bead motion near the animal (Fig. 5). This preference for nearby objects is shown in the normalized histogram in Figure 6A. It is possible, however, that this result, although consistent, may not indicate a true preference for nearby objects, or sensitivity to object distance at all. Because we used a consistent speed for the bead movements, images of nearby objects moved across the retina at higher angular speeds. A preference for higher angular speeds could explain the data as well as a preference for closer objects, as illustrated in the normalized histogram of responses to angular speed (Fig. 6B).

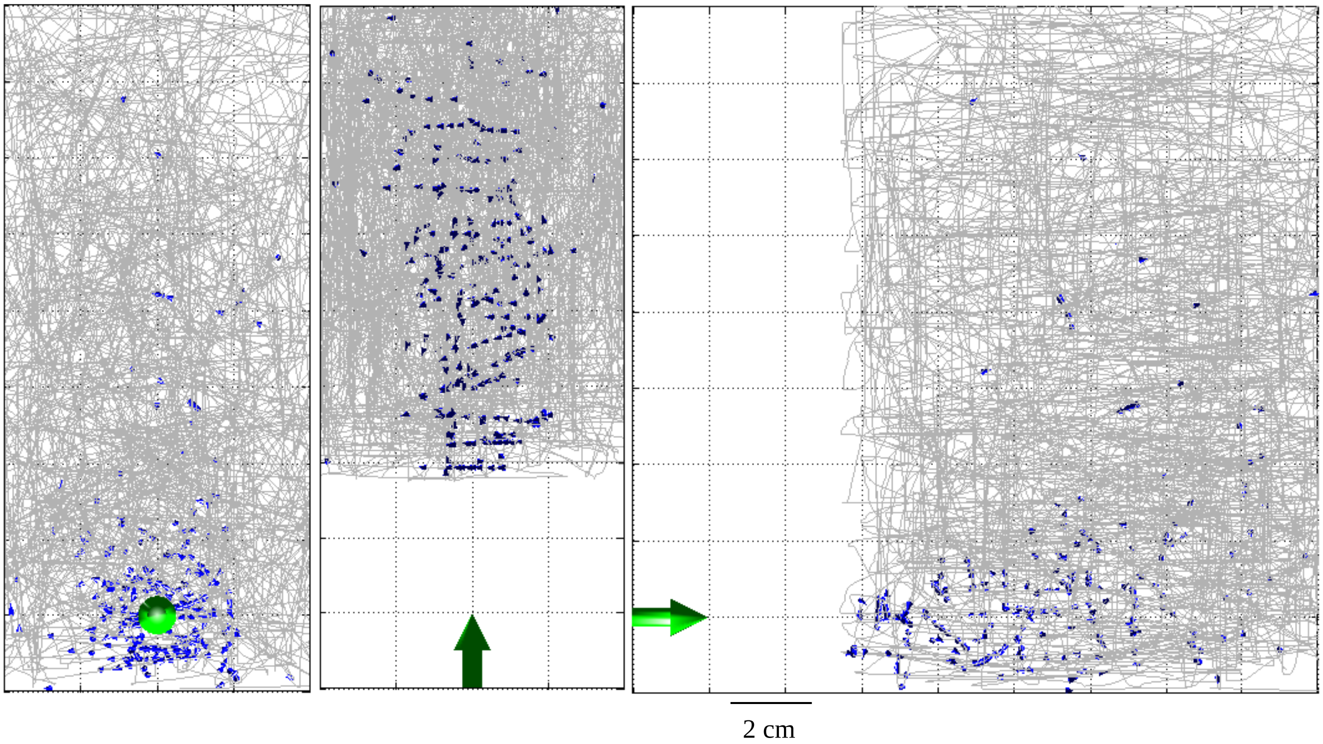

Fig. 5. Receptive field of a TSDN, DIT1, in 3 dimensions. Cones indicate bead location and direction when DIT1 spikes occurred. Gray lines show the entire trajectory of the bead. The locations of the dragonfly's head are indicated by green markers.

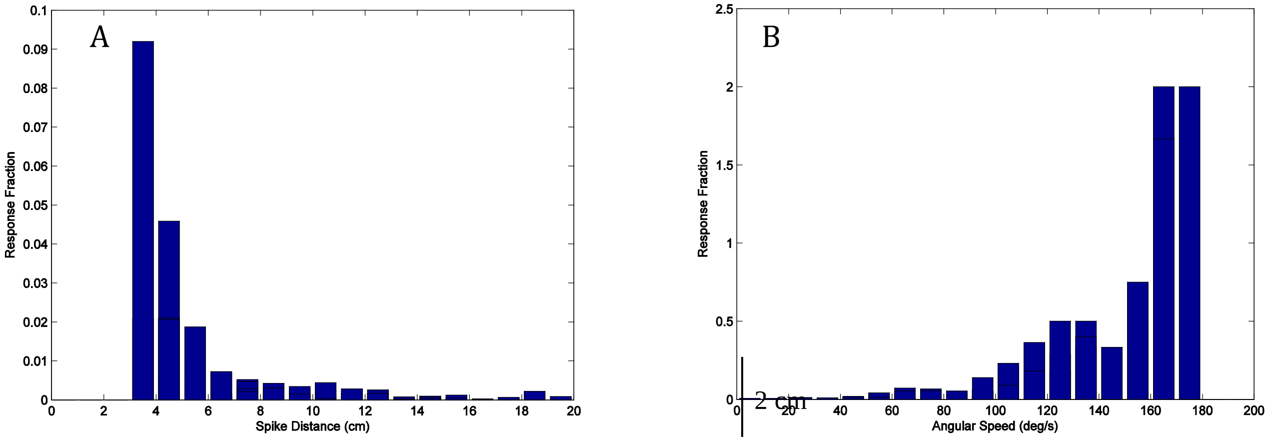

Fig. 6. Normalized histograms of bead angular speed (A) and distance (B) when DIT1 spikes occurred. Data from experiment shown in Fig. 5. This analysis shows that the apparent preference of DIT1 for nearby objects could also be explained by its preference for greater angular speed.

C. TSDN encoding of target speed

We used the prey simulator to test whether the TSDNs encode angular speed. The results, an example of which is shown in Figure 7, show that DIT1, the neuron whose responses are shown in Figure 5, shows a clear preference for higher angular speed, peaking at about 270°/s. And examination of the target speeds that produced the greatest number of spikes (Fig. 6B) is consistent with the speed sensitivity shown in Figure 7.

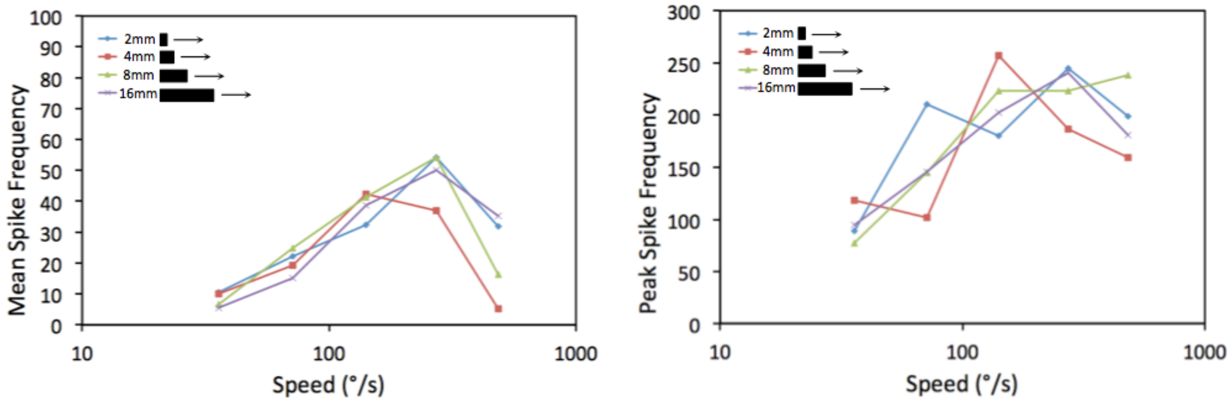

Fig. 7. Responses of DIT1 to black cylindrical objects (4 mm diameter) of varying length, moved along their long axes. Both mean spike frequency (left) and peak spike frequency encode angular speed.

From the above experiments we have no basis for choosing between the following two hypotheses: (1) Heightened TSDN responses to nearby targets could reflect TSDN sensitivity to target distance or (2) The heightened responses could simply reflect TSDN sensitivity to higher angular speeds. To investigate these two possibilities we designed an experiment to control for changes in angular speed with distance. In this experiment we studied TSDN responses to drifting targets projected with a 360 Hz DLP projector onto a screen varying distances from the eyes. The stimuli were designed so that the angular parameters of the stimuli were held constant at different screen distances. For example if the screen distance was doubled the projected target was twice as wide and moved twice as far in the same time. Any differences in responses would thus indicate depth sensitivity in the TSDNs.

Due to the response variability and extreme habituation property of the TSDNs, the results from the variable screen distance experiments were somewhat inconsistent, but in experiments with longer lasting, robust responses, we could detect no distance sensitivity in the TSDNs (Fig. 8)

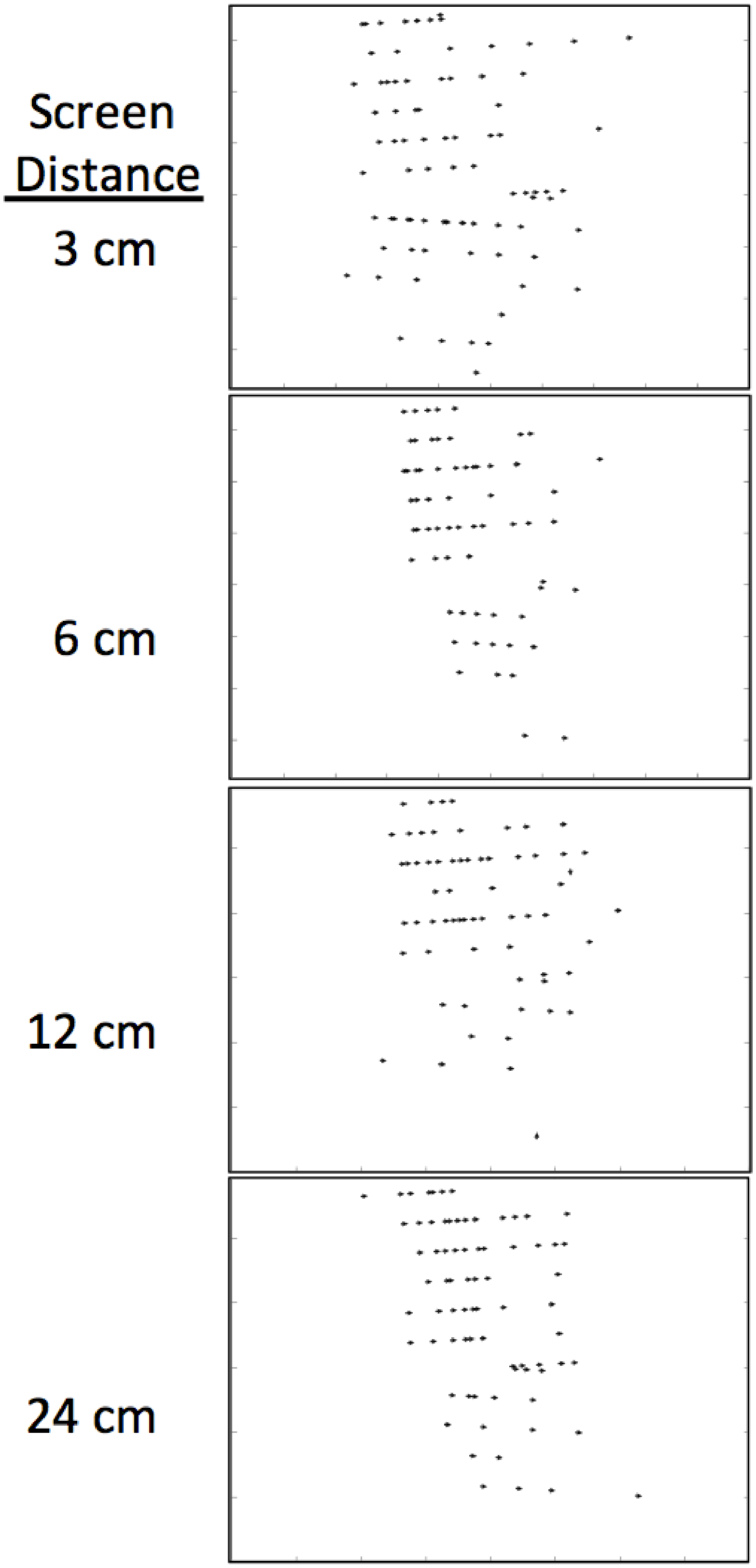

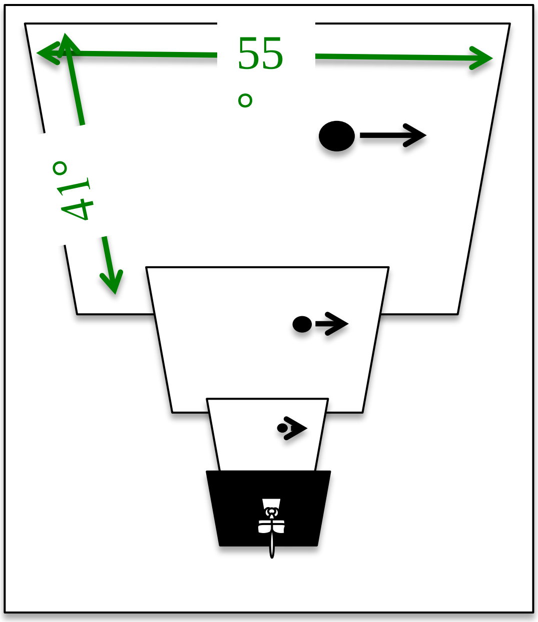

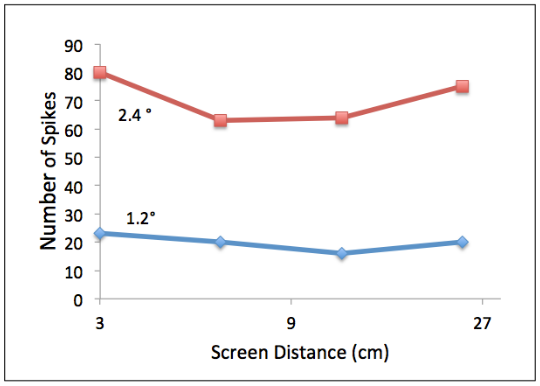

Fig. 8. Lack of sensitivity to object distance in DIT1. Left panel shows spike locations when stimuli with constant angular parameters were presented at different screen distance (as diagrammed at the upper right). Graph above shows similar total spike numbers for two sizes of targets at 4 distances. No preferences for nearby targets can be seen.

With all angular parameters held constant on screens of different distances, the only cue that could be used to detect distance would be the image disparity on the two retinae, i.e. the neurons could employ binocular stereopsis to obtain depth information. Therefore we performed a series of eye-blocking experiments in which the animal viewed the “same” stimuli at 3 different distances (as described above) either with both eyes or with each one eye blocked. The results showed that for TSDNs with midline receptive fields such as DIT1, blocking either eye severely decreases the responses to targets near visual midline (Fig. 9). Thus the summed target responses from the two eyes individually were much smaller than the binocular responses. From these experiments we conclude that integration of binocular input is an important property of at least some of the TSDNs, but the functional significance of the binocular information remains unknown.

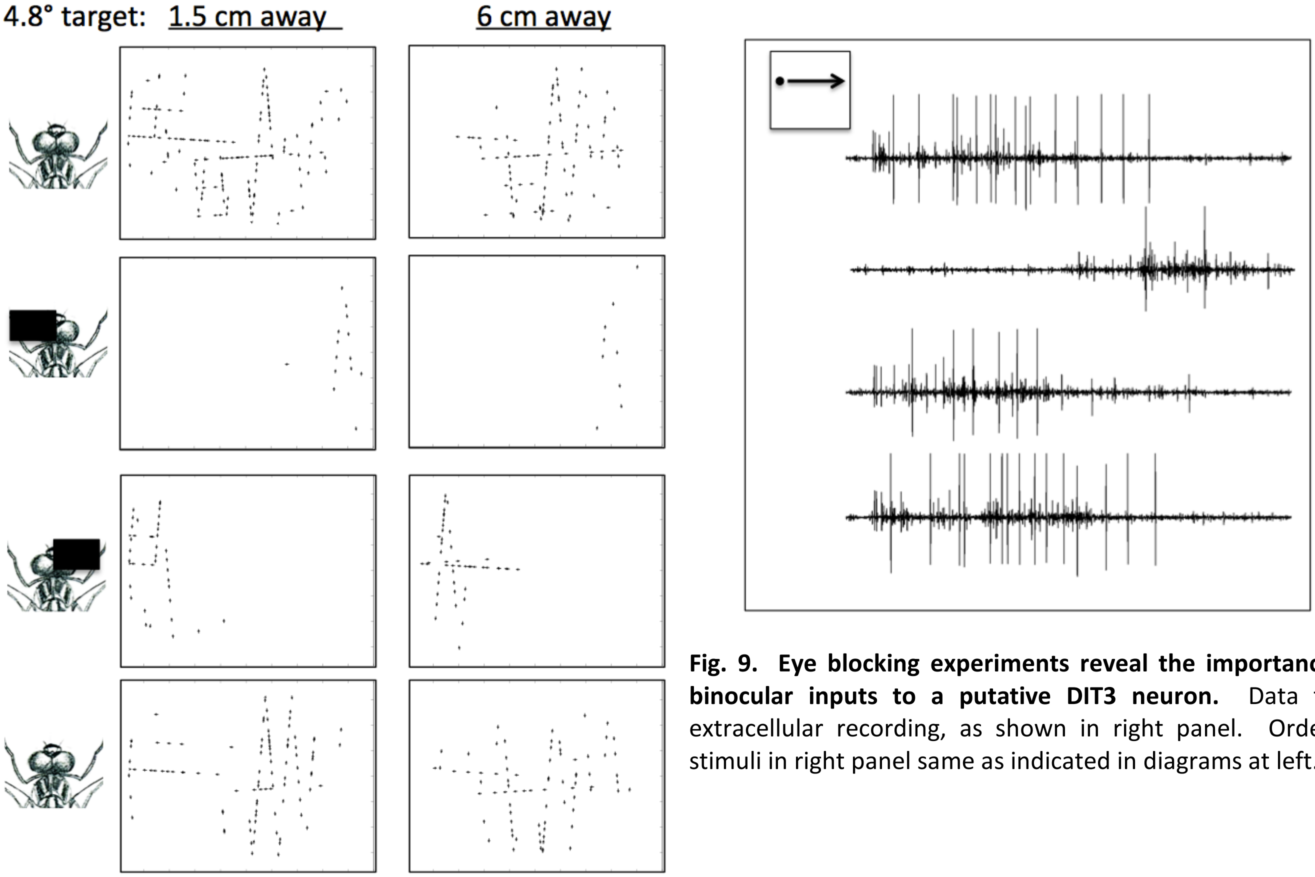

Fig. 9. Eye blocking experiments reveal the importance of binocular inputs to a putative DIT3 neuron. Data from extracellular recording, as shown in right panel. Order of stimuli in right panel same as indicated in diagrams at left.

A further investigation of TSDN responses to target speed was carried out using the DLP projector/screen arrangement, which is a much brighter stimulus, approximating the brightness of midday blue sky. The results showed much higher speed sensitivity than that measured with bead movement with the 3D prey simulator, with increasing speed eliciting increasing spike frequency even beyond 1000 °/s (Fig. 10A). Even at very high speeds, the responses are still clearly directionally selective, indicating that they are truly velocity responses, rather than simply responses to flashing light (Fig 10B). Thus, as shown in Fig 10C, the higher spike rates seen in response to closer targets can easily be explained by TSDN sensitivity to target speed.

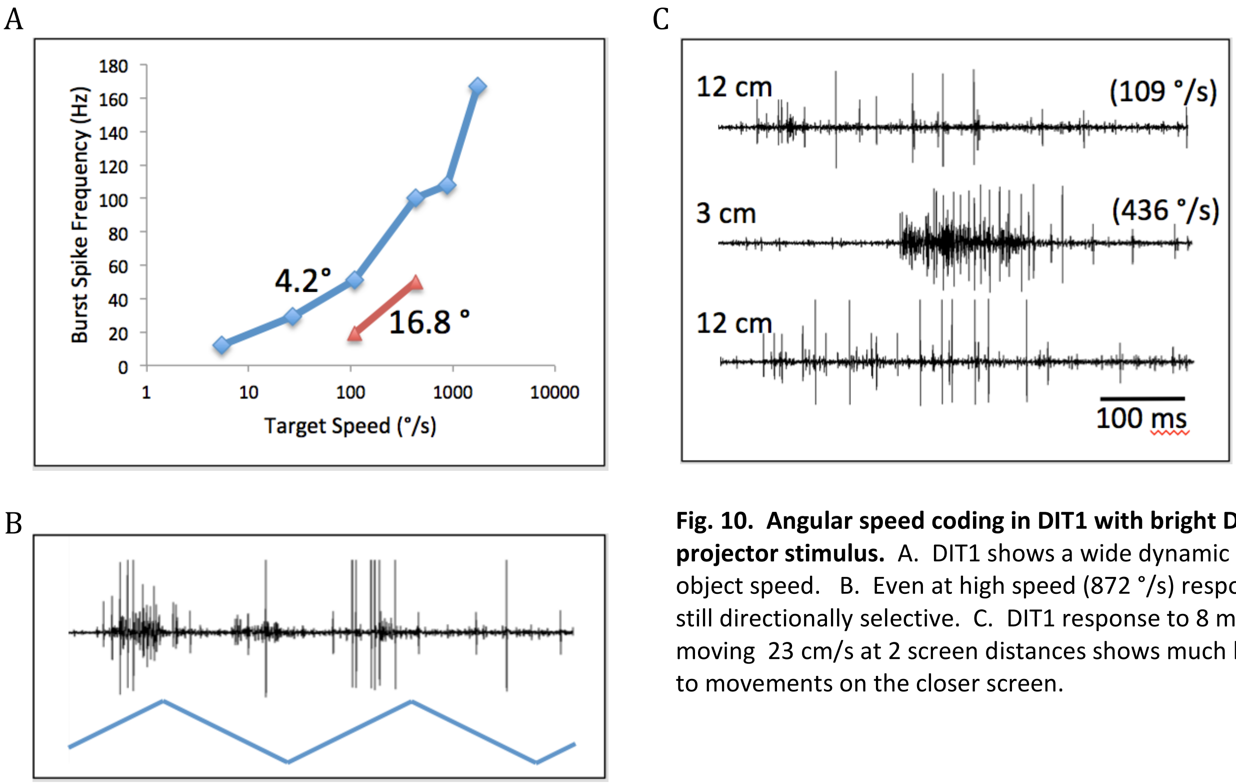

Fig. 10. Angular speed coding in DIT1 with bright DLP projector stimulus. A. DIT1 shows a wide dynamic range to object speed. B. Even at high speed (872 °/s) responses are still directionally selective. C. DIT1 response to 8 mm target moving 23 cm/s at 2 screen distances shows much higher rate to movements on the closer screen.

D. Conclusions and future directions for electrophysiological study

The data summarized above shows that both components of the target velocity vector, direction and speed, are coded by the TSDNs. Because during prey-pursuit behavior nearby target movement will naturally will result in higher angular speeds than more distant target movement, the sensitivity of the TSDNs to speed will presumably serve to increase the gain of the steering system as the dragonfly draws nearer to its prey.

Whether there is some component of TSDN visual responsiveness that is sensitive to target distance is still an open question, although the evidence available to date leads us to conclude that distance is not coded by these cells. However, the importance of binocular inputs to individual TSDNs such as DIT1 would most easily be explained as a mechanism for distance measurement by triangulation between the two eyes. The separation of pseudopupils between the 2 eyes would be sufficient to mediate distance estimation up to about 20 cm (Olberg et al. 2005). However our experiments with varying screen distance showed no consistent discrimination among target distances.

Binocular inputs could be important for precise information about looming objects, i.e. approaching prey, especially those that are near to, and on a collision course with, the head. Information about time to contact appears to be available to the foraging dragonfly, as the legs are consistently thrust forward and upward about 20 ms before contact with the prey (Worthington and Olberg, unpublished). Two TSDNs, DIT3 and MDT3 are sensitive to expanding figures whose time course of expansion simulates looming objects. We hypothesize that these neurons provide at least of some of the time-to-contact information. A high-priority series of experiments to be conducted this year is to record the response of these two neurons to real approaching objects with individual eyes blocked versus with both eyes uncovered. If, as we hypothesize, these cells use binocular information to provide an important timing signal for prey grasping, we predict that blocking either eye will eliminate the burst of spikes to an approaching target.

Finally, It is important to consider a limitation in the results from single-cell electrophysiology presented here. We have shown behaviorally that the dragonfly can discriminate distances beyond 1 meter, i.e. beyond any possibility for triangulation by the two eyes (Olberg et al. 2005). We hypothesized that this discrimination relies on parallax motion cues from head movements. Because the head was always rigidly fixed during our experiments, we could not have recorded any distance sensitivity that relied on head movements.

2. Motor outputs of the TSDNs

A. Wing movements

The dye injection experiments of Gonzalez-Bellido et al. (2012) showed that output arborizations of individual TSDNs are remarkably consistent from animal to animal but differ from one TSDN type to another (Fig. 3). Many experiments have shown that every TSDN forms synapses with its downstream targets that are of sufficient strength to individually drive wing movements. The wing movements driven by TSDN activity vary from making very small adjustments of wing position to driving wing flapping activity. Technical difficulties have made it difficult to produce a complete characterization of the wing movements elicited by each of the TSDNs, identified unequivocally with fluorescent dye injection, and this has not yet been accomplished.

Our working hypothesis is that each TSDN acts on the wing control system to produce flight turns in the direction in its preferred target-movement direction. Thus TSDN activity would serve to turn the animal to compensate for prey drift, minimizing changes in bearing from the dragonfly to its prey., maintaining the prey at a nearly constant bearing assures interception. Clearly the prey interception scenario is not that simple, especially because of target-fixating head movements, which will be discussed below. However it still reasonable to assume that, if the TSDNs are involved in driving prey pursuit (and it is difficult to imagine that they are not), they should turn the animal to follow prey deviations. It remains an important, but challenging, project to detail how this is done at the level of individual neurons and individual wings, both at rest and during flapping flight.

B. Movements of the head and other body parts

In the last year we have developed a new preparation to investigate whether the TSDNs have other motor outputs beyond those to the wings. Anatomical evidence, specifically the axonal arborizations of TSDNs in the subesophageal ganglion and the prothoracic ganglion, suggested that the TSDNs might play a role in head movement in addition to their role in wing movement. The difficulty in determining whether TSDNs move other parts of the body is that the body must be left free to move during microelectrode penetration of individual axons. However intracellular penetration and stimulation requires extreme stability, which is generally obtained by immobilizing all parts of the body as much as possible.

Our approach in developing this new preparation was to affix the animal at only one point (behind the metathoracic legs), leaving the wings, head, prothoracic segment and prothoracic legs free to move while we attempted to penetrate TSDNs in the ventral nerve cord near their posterior end, i.e. between the meso- and meta-thoracic ganglia. The rationale in this approach was that if TSDN activity indeed produced head movement, the region posterior to the mesothoracic ganglion is the only place where the nerve cord itself would not be actively moved by TSDN-driven muscle activity.

In about 48 preparations we have succeeded in driving TSDN activity in only 5 cases, but the results from these limited successes are consistent. TSDN activity drives head movement and in some cases leg movement and even movement of the mouthparts. From these sparse results two important generalities emerge: (1) The head is moved in the direction roughly <u>opposite</u> to the neuron's preferred target movement direction (Fig. 11), and (2) the neurons that respond especially well to looming targets (MDT3 and DIT3) also move the front legs and open the mouth. It seems likely that these neurons move all of the legs, but this is uncertain because the other legs must be removed to expose the recording site.

What is the significance of TSDN-induced head rotation in the direction away from the target vector that excites the neuron? If, as we hypothesize, TSDN-driven wing movements turn the animal in the direction of the target movement, the head would need to rotate in the opposite direction to maintain target fixation on the retina. Two studies (Olberg et al. 2007 & Mischiati et al. – submitted to *Nature*) show that during prey interception flights the image of the prey is fixed on the "crosshairs" formed by the vertically oriented visual midline and the horizontally oriented dorsal acute zone – or fovea - of the compound eyes. Targets are continuously fixated within a few degrees of this highly acute visual center *in real time*, i.e. with no visual latency. For this to occur, any turn of the animal must be accompanied by a simultaneous counterturn of the head. The most parsimonious scheme for accomplishing this counter-rotation is for the same neurons to drive both wing and head movements, a function that we now ascribe to the TSDNs.

The observation that the activity of looming sensitive neurons also drives mouthpart and leg movement suggests a highly efficient coordination of behavioral components. The looming-sensitive TSDNs, MDT3 and DIT3, produce a burst of spike activity during the *ca.* 100 ms period before contact with the approaching object (prey). During this period the legs are extended into a basketlike arrangement to ensnare the prey and mouth is opened to accept it. Our results indicate that an entire suite of behaviors, wing steering, head rotation, leg extension and mouth preparation is driven, at least in part, by an extremely small set of large neurons.

C. Conclusions and future directions

We now have consistent and convincing evidence that the TSDNs are truly master cells in controlling behavior. A single TSDN is capable of driving a suite of behaviors including the movement of all four wings, rotation of the prothoracic segment and head, leg movement and even movement of the

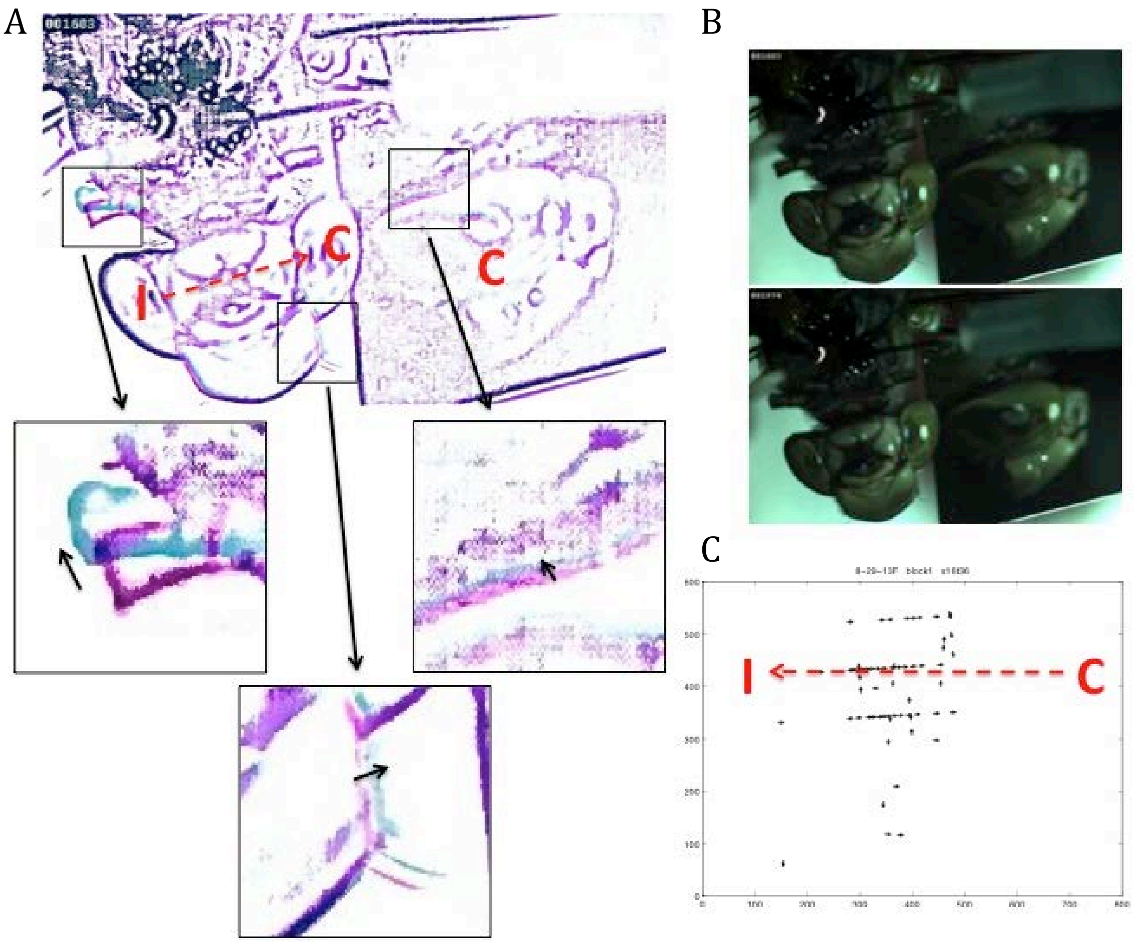

Fig. 11. Head and leg movements elicited by left MTD2. A. Superimposed line drawings extracted from the video frames shown in B. Magenta lines show head and leg contours before stimulation. Blue lines show contours during 250 Hz spiking of MDT2. Magnified insets show backward movement of the left (Ipsilateral) prothoracic leg and head yaw to the right (Contralateral) side – as indicated by red dashed arrow from Ipsilateral to Contralateral. B. Video frames used in A.
C. Receptive field of the left MDT2 neuron. Arrows represent position of black 3.6° circular target when each MDT2 spike occurred, pointing in direction of target motion on the projection screen. REceptive field map shows that the preferred direction of target motion for this neuron was from right (Contralateral) to left (Ipsilateral). **I** is Ipsilateral and **C** is Contralateral, relative to the intracellularly stimulated MDT2 neuron.

mouthparts. Of particular interest is the finding that the rotation of the head is in the *opposite* direction from the TSDN's preferred target direction. This is completely consistent with real-time gaze stabilization against the dragonfly's own turning movements. Documenting and quantifying all of the movements elicited by TSDN stimulation is now a very high priority goal. Accomplishing this will reveal the way in which a small group of neurons is capable of driving a wide range of coordinated movement.

3. Wireless recording of TSDN activity during prey interception

This project, in collaboration with Anthony Leonardo (HHMI, Janelia Farm), Reid Harrison (Intan Technologies, Los Angeles) and others was aimed at placing a small, lightweight amplifier/transmitter unit (Harrison et al. 2011) on a free-flying dragonfly to amplify and relay the activity of individual

TSDNs from a recording electrode during flight. A custom-fabricated electrode was implanted in the dragonfly's thorax, wrapping around the nerve cord and bearing contacts designed to monitor the extracellular activity of the TSDNs. During the granting period, development of the wireless telemetry chip has moved forward, with the battery being replaced first by a laser-powered photodiode array and most recently by RFID power (Thomas, et al. 2012) resulting in a remarkably lightweight (38 mg) unit.

I terminated my visiting-scientist appointment at Janelia Farm in 2012 when I realized that I had very little to contribute to this project while the telemetry chip was under development. Although we succeeded in wireless recording of neuronal activity of dragonflies perched in the indoor flight arena at Janelia Farm, we were not successful in inducing animals with implanted electrodes and carrying the telemetry chip to take off in pursuit of prey.

When it is successfully accomplished, wireless recording of TSDN activity has the potential to answer questions that cannot by answered in any other way. To monitor the small number of TSDNs that are believe to steer complex interception flight behavior will reveal whether, as seems likely, a very sparse code is used by these neurons with very few spikes, but very precise timing driving successful prey interception and capture.

4. Grant Supplement for Killer Fly Prey Interception Study

A. Introduction

A supplement to this grant provided funding for a pilot study for Drs. Paloma Gonzalez-Bellido and Trevor Wardill to investigate prey interception flights by killer flies (*Coenosia attenuata*). These small flies routinely grab other flies, such as fruit flies (*Drosophila*) in mid-flight, even though the prey are nearly the same size as the predator. The grant supplement funded the rental of high-speed video cameras to record and reconstruct interception flights in three dimensions. This work was done in the field in southern Spain.

B. Goals accomplished

1. Successful development of a custom right angle support system for two synchronized high-speed video cameras (Fig. 12A&B).

2. Obtained high-speed video recordings to reconstruct, in 3D, the flight trajectory of an aerial predator (killer fly: *C. attenuata*) and its potential prey (small flying insects such as fungus gnats, white flies, fruit flies...etc) in their "wild" environment (large greenhouses in Spain) and in captivity.

3. Confirmed that killer flies do not estimate absolute bead size before take off, and thus they can be tricked into chasing a bead that is three times their body size. (Fig. 12C).

4. Confirmed that killer flies display an interception trajectory, and identifying such strategy as 'Partial lead' (Fig. 13).

5. Confirmed that killer flies are most likely to take off after a target moving between 0.5 and 1.2 m/s, when the target was 3mm in diameter and at an average distance of 10cm. This is in accordance with the average flight speed of the fruit fly, which is approximately 0.5. - 1m/s and the distance parameters recorded in the wild.

6. Determined that the minimum reaction time recorded between prey movement and killer fly movement was 33 ms, which is on par with the reaction time of other predatory insects, such as dragonflies.

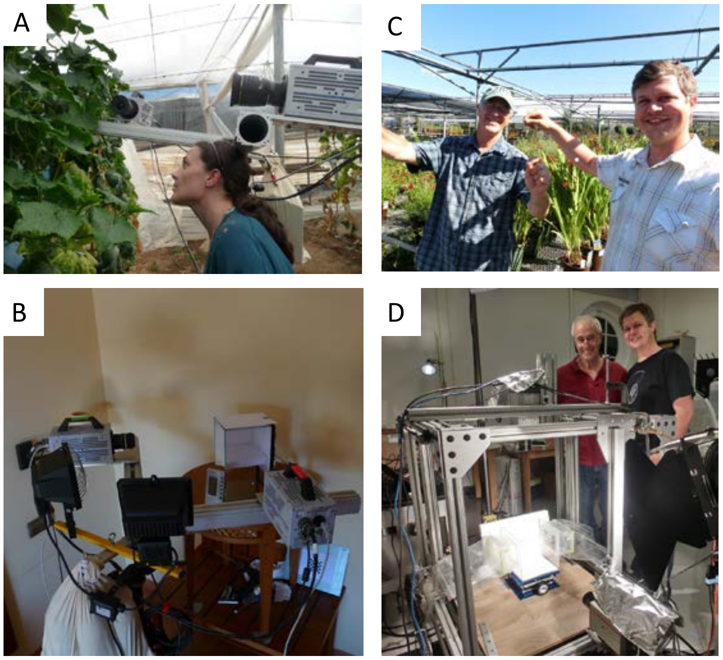

Figure 12. Recording killer fly aerial attacks with high-speed video cameras in the field (A) and in captivity (B), in Spain. Further field carried out in Cape Cod (MA) to test the effect of bead size(C), and in the Olberg Laboratory (Union College, NY) to test the effect of bead speed by controlling the bead with a computer and motors (D).

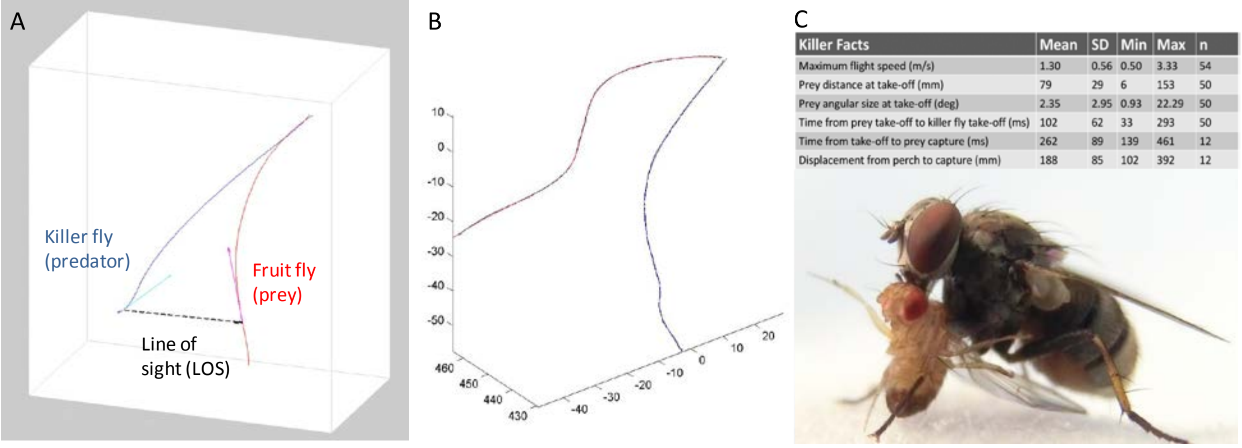

Killer Facts	Mean	SD	Min	Max	n
Maximum flight speed (m/s)	1.30	0.56	0.50	3.33	54
Prey distance at take-off (mm)	79	29	6	153	50
Prey angular size at take-off (deg)	2.35	2.95	0.93	22.29	50
Time from prey take-off to killer fly take-off (ms)	102	62	33	293	50
Time from take-off to prey capture (ms)	262	89	139	461	12
Displacement from perch to capture (mm)	188	85	102	392	12

Figure 13. Flight strategy of Killer flies in the wild and in captivity. By digitizing the predator and prey trajectories in 3D, and using the software provided by the Krishnaprasad laboratory to reconstruct trajectories, we confirmed that killer flies use a type of interception trajectory seen in fighter plane combat, termed 'Partial lead'. We have observed killer flies displaying this behavior in the wild (A) and in captivity (B). We picked 12 wild trajectories and 6 captivity trajectories that were relatively simple to understand and analyze (i.e. the flight path was not convoluted) Such data set yielded the data shown in (C).

References

Frye, MA and Olberg, RM (1995) Receptive field properties of feature detecting neurons in the dragonfly. J.Comp.Physiol. A 177:569-576

Gonzalez-Bellido PT, Penga H, Yanga J, Georgopoulos A,and Olberg RM (2012). Eight pairs of descending visual neurons in the dragonfly give wing motor centers accurate population vector of prey direction. PNAS **110**(2):696-701

Harrison RR, Fotowat H, Chan R, Kier RJ, Olberg R, Leonardo A. and Gabbiani F. (2011) Wireless Neural/EMG Telemetry Systems for Small Freely Moving Animals. IEEE Trans Biomed Circ. Syst. 5(2):103-111.

Olberg, RM (1981) Parallel encoding of direction of wind, head, abdomen, and visual pattern movement by single interneurons in the dragonfly. J. Comp. Physiol. 142:27-41.

Olberg, RM (1986) Identified target-selective visual interneurons descending from the dragonfly brain. J. Comp. Physiol. 159:827-840.

Olberg, RM, Worthington AH, Fox JL, Bessette CE, Loosemore MP (2005). Prey size selection and distance estimation in foraging adult dragonflies. J Comp Physiol A 191:791-797

Olberg RM, Seaman RC, Coats MI, Henry AF. (2007) Eye movements and target fixation during dragonfly prey-interception flights. J Comp Physiol A 193:685-693.

Thomas S, Harrison R, Leonardo A, and Reynolds M (2012) A Battery-Free Multi-Channel Digital Neural/EMG Telemetry System for Flying Insects, IEEE Transactions on Biomedical Circuits and Systems. **6**(5):424-436.